POLITECNICO DI TORINO
Repository ISTITUZIONALE

Data-driven nonlinear model reduction by moment-matching for the ISWEC system

(Article begins on next page)

02 September 2025

Data-driven nonlinear model reduction by moment-matching for the ISWEC system

1st Nicolás Faedo
Marine Offshore Renewable Energy Lab,
Politecnico di Torino
Turin, Italy
nicolas.faedo@polito.it

2st Francisco Javier Dores Piuma
Departamento de Ciencia y Tecnología
Universidad Nacional de Quilmes
Bernal, Argentina

3st Giuseppe Giorgi
Marine Offshore Renewable Energy Lab,
Politecnico di Torino
Turin, Italy

4st Giovanni Bracco
Marine Offshore Renewable Energy Lab,
Politecnico di Torino
Turin, Italy

5st John V. Ringwood
Centre for Ocean Energy Research,
Maynooth University
Maynooth, Ireland

6st Giuliana Mattiazzo
Marine Offshore Renewable Energy Lab,
Politecnico di Torino
Turin, Italy

Abstract—**Given the relevance of control-oriented models in optimal control design for wave energy converters (WECs), this paper presents a *data-driven* technique to achieve nonlinear model reduction by *moment-matching* for the ISWEC device, a device originally developed at the Politecnico di Torino. The presented model reduction technique is capable of providing simple WEC models, which intrinsically preserve steady-state behaviour from the target nonlinear system, by merely using information on the system outputs, defined for a set of operating conditions. We demonstrate that the proposed model reduction by moment-matching procedure is well-posed for the ISWEC, and illustrate the efficacy of this reduction technique under a variety of sea conditions.**

Index Terms—**Wave energy, model reduction, nonlinear systems, optimal control**

I. Introduction

Wave energy converters (WECs) need to be controlled to maximise the energy absorbed from incoming waves, hence reducing the associated levelised cost of energy [1], [2]. Both performance and computational burden associated with such control algorithms depend upon the availability of *control-oriented* models, capable of providing a suitable trade-off between accuracy and complexity [3]. An effective pathway towards computation of such models is via *model reduction*.

A particularly well-developed WEC system is the so-called ISWEC device [4], originally proposed by the Politecnico di Torino (see Figure 1). Motivated by the intrinsic nonlinear behavior of this device [5], and the underlying necessity of reduced models for optimal control design, the objective of this paper is to produce reliable and computationally efficient reduced models by *moment-matching* [6], [7] for the ISWEC system, under a variety of input conditions.

The model reduction by moment-matching framework produces models such that their associated steady-state responses

match the steady-state behaviour of the desired system to be reduced. We note that a step has been taken in [8] to solve the model reduction by moment-matching problem for WECs under hydrodynamic nonlinearities, though the strategy inherently necessitates the solution of a nonlinear system of algebraic equations, which might not be feasible for systems with complex power-take off (PTO) systems, such as the ISWEC.

In the light of this, we propose, in this paper, a *data-driven* approach to nonlinear model reduction for the ISWEC system, inspired by the results in [9]. To that end, we show existence and uniqueness of the associated moment for the ISWEC case, and propose an algorithm to estimate such a mapping using only knowledge of the WEC outputs, for a certain class of input signals of interest. Furthermore, we fully illustrate the effectiveness of the strategy in terms of a detailed case study.

This manuscript is organised as follows. Section II recalls the notion of a model reduced by moment-matching, while Section III discusses the dynamics of the ISWEC device. Section IV discusses theoretical aspects behind the definition of moment for ISWEC, while Section V presents a data-driven procedure to compute an approximation of the associated moment. With such an approximation, Section VI illustrates the performance of the proposed methodology, for a regular sea-state, with a large variation in terms of wave height. Finally, Section VII encompasses the main outcomes of our study. Note that we do not explicitly provide proofs of our theoretical results for economy of space. These are to be presented in an extended version of this manuscript.

II. Preliminaries on moment-matching

This section recalls standard results in moment-based model reduction. The interested reader is invited to consult [6], [7], for a thorough discussion of the topic. Let Σ be a nonlinear,

single-input single-output (SISO) system, given by the set of equations[1]

$$\Sigma : \{\dot{x} = f(x, u), \ y = h(x), \tag{1}$$

with $x(t) \in \mathbb{R}^n$, $\{u(t), y(t)\} \subset \mathbb{R}$, and sufficiently smooth mappings f and h such that $f(0,0) = 0$ and $h(0) = 0$. Assume system (1) is *minimal*. Consider now a *signal generator*, *i.e.* an implicit form description of u, characterised by

$$\dot{\xi} = W\xi, \ u = Q\xi, \tag{2}$$

with $\{\xi(t), Q^{\intercal}\} \subset \mathbb{R}^{\nu}$, $W \in \mathbb{R}^{\nu \times \nu}$, and the composite dynamical system

$$\dot{\xi} = W\xi, \ \dot{x} = f(x, Q\xi), \ y = h(x). \tag{3}$$

We now introduce a set of standard assumptions in moment-based theory.

Assumption 1. $(Q, W, \xi(0))$ is minimal.

Assumption 2. The matrix W in (2) is such that $\lambda(W) \subset \mathbb{C}^0$ with *simple* eigenvalues.

The following main result holds (see [6], [7]).

Lemma 1. [6], [7] *Let Assumption 1 and Assumption 2 hold Suppose the zero equilibrium of system (1) is locally exponentially stable. Then, the invariance equation*

$$\frac{\partial \pi(\xi)}{\partial \xi} W\xi = f(\pi(\xi), Q\xi), \tag{4}$$

has a unique locally defined solution π, $\pi(0) = 0$. Furthermore, the steady-state response of the interconnected system (3) is $x_{\mathrm{ss}}(t) = \pi(\xi(t))$, for any set of sufficiently small initial conditions $\{x(0), \xi(0)\}$.

Remark 1. The mapping π is of class $\mathcal{C}^r$, with $r \geq 1$ [10].

Definition 1. [6], [7] The mapping $h \circ \pi$ is termed the *moment* of system (1) at the signal generator (2), *i.e.* at (W, Q).

Remark 2. Since $h(0) = 0$ by assumption, the moment $h \circ \pi$ is always such that $h(\pi(0)) = 0$.

A. Model reduction by moment-matching

Model reduction by moment-matching is based upon the idea of interpolating the steady-state response of a given system, by means of Definition 1. To be precise, a family of reduced models by moment-matching for system (1) can be defined [6] as

$$\tilde{\Sigma} : \left\{ \dot{\Gamma} = (W - \delta(\Gamma)Q)\Gamma + \delta(\Gamma)u, \ \gamma = h(\pi(\Gamma)), \tag{5} \right.$$

with $\delta : \mathbb{R}^{\nu} \to \mathbb{R}^{\nu}$ a free (user-defined) mapping. The determination of $\tilde{\Sigma}$ depends upon the computation of the mapping $h \circ \pi$, solution of (4). The latter is far from being trivial, even with full knowledge of the mappings f and h in (1), given the nature of (4). This issue is specifically tackled using a data-driven approach, in Section V.

[1]The dependence on t is dropped when clear from the context.

III. ISWEC DYNAMICS

The ISWEC system, schematically depicted in Figure 1, is composed of a hull which incorporates a gyroscope and a power take-off (PTO) axis, commonly termed ε-axis, which transforms the associated gyroscopic motion into electricity. We consider that the hull of the device is constrained to move in pitch (which is the degree-of-freedom where most energy from incoming waves is absorbed) and, hence, the associated dynamics can be described by the set of coupled equations:

$$\begin{cases} I_p \ddot{z} + k_{\mathrm{r}} \ast \dot{z} + s_h z - J\psi\dot{\varepsilon}\cos(\varepsilon) = \tau_{\mathrm{e}}, \\ I_g \ddot{\varepsilon} + J\psi\dot{z}\cos(\varepsilon) - \tau_{\mathrm{PTO}}(\varepsilon) = 0, \end{cases} \tag{6}$$

with $z : \mathbb{R}^+ \to \mathbb{R}$, $t \mapsto z(t)$, denoting the (rotational) displacement in pitch, and where $\varepsilon : \mathbb{R}^+ \to \mathbb{R}$, $t \mapsto \varepsilon(t)$ denotes the gyroscope precession angle.
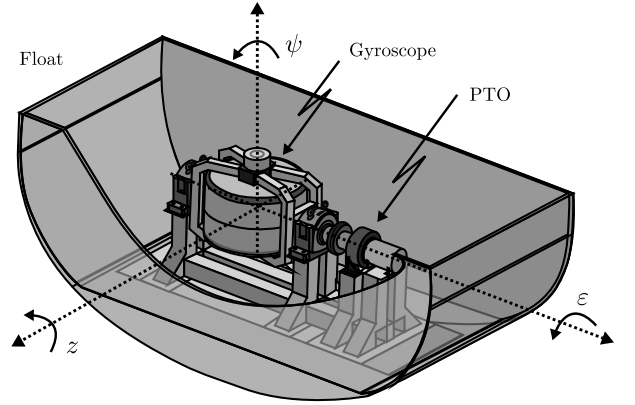

Fig. 1. Schematic illustratation of the ISWEC device, developed at Politecnico di Torino (figure adapted from [11]).

The wave excitation torque is denoted by $\tau_{\mathrm{e}} : \mathbb{R}^+ \to \mathbb{R}$, $t \mapsto \tau_{\mathrm{e}}(t)$. The function $k_{\mathrm{r}} \in L^2(\mathbb{R})$, $t \mapsto k_{\mathrm{r}}(t)$, is the impulse response mapping associated with memory effects arising from the fluid response, while $s_h \in \mathbb{R}$ is the so-called hydrodystatic stiffness. The set of parameters $\{I_p, J, I_g\} \subset \mathbb{R}^+$ denote the inertia of the device in pitch (including the so-called added-inertia at infinite-frequency [12]), gyroscopic inertia, and total moment of inertia in the ε-axis, respectively. Finally, $\psi \in \mathbb{R}^+$ denotes the (suitably selected - see [5]) constant value for the flywheel speed. The PTO moment τ_{PTO} is chosen here based upon a proportional-derivative (PD) control strategy, *i.e.*

$$\tau_{\mathrm{PTO}}(\varepsilon) = -k_{\mathrm{PTO}}^{\varepsilon}\varepsilon - k_{\mathrm{PTO}}^{\dot{\varepsilon}}\dot{\varepsilon}, \tag{7}$$

with $\{k_{\mathrm{PTO}}^{\varepsilon}, k_{\mathrm{PTO}}^{\dot{\varepsilon}}\} \subset \mathbb{R}$. This set of parameters is commonly computed such that the energy absorption from waves is maximised, while minimising chances of actuator/device damage. The impulse response function k_{r} is approximated [13] in terms of a finite-dimensional dynamical structure, *i.e.*

$$\dot{p} = Fp + G\dot{z}, \ k_{\mathrm{r}} \ast \dot{z} \approx Hp, \tag{8}$$

with $p(t) \in \mathbb{R}^{n_{\mathrm{r}}}$, and where the set of real-valued matrices (F, G, H) are dimensioned accordingly.

With the approximation defined in (8), the set of equations (6) can be written analogous to (1) as follows:

$$\Sigma : \left\{ \dot{x} = f(x, \tau_e) = Ax + B\tau_e + g_{nl}(x), \ y = h(x) = Cx, \right. \tag{9}$$

where the state-vector is defined as $x = [z \ \dot{z} \ \varepsilon \ \dot{\varepsilon} \ p^\intercal]^\intercal$, $x(t) \in \mathbb{R}^{4+n_r}$, and the triple of matrices (A, B, C), and mapping g_{nl}, are given by the expressions below:

$$A = \begin{bmatrix} A^0 & -B^0 H \\ GC^0 & F \end{bmatrix}, \ B = \begin{bmatrix} B^0 \\ 0 \end{bmatrix},$$
$$C = \begin{bmatrix} C_\varepsilon & 0 \end{bmatrix}, \ g_{nl}(x) = \begin{bmatrix} g^0(x) \\ 0 \end{bmatrix}, \tag{10}$$

together with

$$A^0 = \begin{bmatrix} 0 & 1 & 0 & 0 \\ -\frac{s_h}{I_p} & 0 & 0 & 0 \\ 0 & 0 & 0 & 1 \\ 0 & 0 & -\frac{k_{PTO}^\varepsilon}{I_g} & -\frac{k_{PTO}^{\dot{\varepsilon}}}{I_g} \end{bmatrix}, \ B^0 = \begin{bmatrix} 0 \\ \frac{1}{I_p} \\ 0 \\ 0 \end{bmatrix},$$

$$C^{0\intercal} = \begin{bmatrix} 0 \\ 1 \\ 0 \\ 0 \end{bmatrix}, \ C_\varepsilon^\intercal = \begin{bmatrix} 0 \\ 0 \\ 1 \\ 0 \end{bmatrix}, \ g^0(x) = \begin{bmatrix} 0 \\ \frac{J\psi}{I_p} x_4 \cos(x_3) \\ 0 \\ -\frac{J\psi}{I_g} x_2 \cos(x_3) \end{bmatrix}, \tag{11}$$

where $A \in \mathbb{R}^{4+n_r}$, $\{B, C^\intercal\} \subset \mathbb{R}^{4+n_r}$, $A^0 \in \mathbb{R}^{4\times4}$, $\{B^0, C^{0\intercal}, C_\varepsilon^\intercal\} \subset \mathbb{R}^4$. Note that the smooth mappings g_{nl} and g^0 are such that $g_{nl} : \mathbb{R}^{4+n_r} \to \mathbb{R}^{4+n_r}$ and $g^0 : \mathbb{R}^{4+n_r} \to \mathbb{R}^4$, and where $g_{nl}(0) = 0$ and $g^0(0) = 0$.

IV. Moment-based analysis for the ISWEC device

We show, in this section, that the moment for the ISWEC system, computed at the class of input signals arising in wave energy applications, is always well-defined, and we expose fundamental properties behind $h \circ \pi$. These results are exploited later in the proposed data-driven algorithm, in Section V.

Following the theoretical results recalled in Section II, τ_e is expressed in terms of a corresponding exogeneous system, i.e.[2]

$$\dot{\xi} = W\xi, \quad \tau_e = Q\xi, \quad W = \begin{bmatrix} 0 & \omega_0 \\ -\omega_0 & 0 \end{bmatrix}, \tag{12}$$

for $t \in \mathbb{R}^+$, with $\{\xi(t), Q^\intercal\} \subset \mathbb{R}^2$, $\omega_0 \in \mathbb{R}^+$.

From now on, and without any loss of generality, $Q^\intercal = [1 \ 1]$. Note that $([1 \ 1], W, \xi(0))$ is minimal as long as $(W, \xi(0))$ is excitable (reachable).

Remark 3. With any $\xi(0)$ such that $(W, \xi(0))$ is excitable, one can automatically check that span$\{\xi_1, \xi_2\} =$ span$\{\cos(\omega_0 t), \sin(\omega_0 t)\}$. In other words, the mapping τ_e is always T_0-periodic, where the so-called *fundamental period* is given by $T_0 = 2\pi/\omega_0 \in \mathbb{R}^+$.

Throughout the reminder of this section, we prove existence of the moment of system (9) at the signal generator defined by (12), which guarantees well-posedness of the model reduction

by moment-matching procedure for the ISWEC device. To do so, we introduce the following assumption on system (9).

Assumption 3. The zero equilibrium of the ISWEC system, i.e. $\dot{x} = f(x, 0)$, with f as in (9), is locally exponentially stable.

Lemma 2. *Consider the ISWEC system* (9) *and the exogenous system* (12). *Let* $Q = [1 \ 1]$ *and suppose* $\xi(0) = [\alpha \ \beta]^\intercal$ *is such that* α *and* β *are not simultaneously zero. Suppose Assumption 3 holds. Then, the moment* $h \circ \pi$ *for the ISWEC system at* (W, Q) *is well-defined.*

It follows that a set of (reduced) models achieving moment-matching at (W, Q) of order $\nu = 2$, can be written in terms of the corresponding mapping $h \circ \pi$,

$$\tilde{\Sigma} : \begin{cases} \dot{\Gamma} = (W - \Delta Q)\Gamma + \Delta\tau_e, \\ \tilde{y} = h(\pi(\Gamma)) = C\pi(\Gamma), \end{cases} \tag{13}$$

with the matrix $\Delta \in \mathbb{R}^\nu$ a user-defined parameter.

Remark 4. Note that system (13) is input-to-state *linear*. This is highly appealing in terms of computational terms: the main 'cost' behind solving (13) for a given input signal is merely the cost of solving a linear differential equation, which can be performed very efficiently.

Finally, we present the following result, which is fundamental for the upcoming sections. In particular, we show that the moment, computed along a specific trajectory of (12), is of a T_0-periodic nature.

Lemma 3. *Suppose the triple* $([1 \ 1], W, \xi(0))$ *is minimal and that Assumption 3 holds. Then, the mapping* $h \circ \pi \circ \xi$ *is* T_0-*periodic, with* $T_0 = 2\pi/\omega_0$.

V. Data-driven approximation of $h \circ \pi$

Even with exact knowledge of the system dynamics, i.e. equation (9), the computation of the mapping π in (13) can be a difficult task. Motivated by this, we present a data-driven approach to approximate the corresponding moment, by explicitly using 'measured' outputs of system (9), for different inputs generated by (12), in order to provide a suitable estimate of the mapping $h \circ \pi$. Aiming to simplify the exposition of the upcoming results, we adopt the notation $\mathcal{M} = h \circ \pi$ throughout the reminder of our study. We start by introducing the following standard assumption, which is inspired by [9].

Assumption 4. $\mathcal{M}$ belongs to the space generated by a family of real-valued mappings $\{\zeta_j\}_{j=1}^\infty$, with $\zeta_i : \mathbb{R}^2 \to \mathbb{R}$, $\zeta_i \in \mathcal{C}$, i.e one can always find a set of constants a_j such that $\mathcal{M}(\xi) = \sum_{j=1}^\infty a_j \zeta_j(\xi)$, for every $\xi \in \Xi$.

Assumption 4 provides a natural definition for an approximation of $\mathcal{M}$, as detailed in Definition 2. Note that, in practice, the family of functions ζ_j can be selected via a trial and error procedure, using, for instance, a polynomial expansion.

Definition 2. Suppose Assumption 4 holds. We call the mapping $\tilde{\mathcal{M}}(\xi) = \sum_{j=1}^N a_j \zeta_j(\xi)$, with N finite, the *approximated moment* of system (9) at the signal generator (W, Q).

Definition 2 is based upon the idea of 'truncating' the expansion for $\mathcal{M}$, available upon Assumption 4, up to N basis functions, *i.e.* the moment is essentially approximated by its expansion in the subset $\{\zeta_j\}_{i=1}^N$. In fact, the data-driven approach presented aims to compute the set of coefficients $\{a_j\}_{j=1}^N$ for the ISWEC case, by explicitly using information on the steady-state output response of (9). To achieve this, let us define the following auxiliary variables

$$
\begin{aligned}
\Pi &= \begin{bmatrix} a_1 & a_2 & \dots & a_N \end{bmatrix}, \\
Z(\xi) &= \begin{bmatrix} \zeta_1(\xi) & \zeta_2(\xi) & \dots & \zeta_N(\xi) \end{bmatrix}^\mathsf{T},
\end{aligned}
\tag{14}
$$

where $\{\Pi^\mathsf{T}, Z(\xi)\} \subset \mathbb{R}^N$. Note that, with the definitions presented in (14), the approximated moment can then be written in a compact form as

$$
\tilde{\mathcal{M}}(\xi) = \Pi Z(\xi),
\tag{15}
$$

and hence the approximation problem reduces to find a suitable matrix Π, for a given basis-function vector $Z(\xi)$.

In the following, we define a number of key sets, which are fundamental for the computation of the corresponding approximation. Let us define $\mathscr{I}_0 = \{\xi_0^i\}_{i=1}^{N_t} \subset \mathbb{R}^2$, with each initial condition in $\mathscr{I}_0$ defined as $\xi_0^i = [\alpha_i \, \beta_i]^\mathsf{T}$, where the (sufficiently small) constants α_i and β_i are not simultaneously zero for all $i \in \mathbb{N}_N$. Let $\mathscr{I} = \{\xi^i(t)\}_{i=1}^{N_t} \subset \Xi$ be the associated set of trajectories, where ξ^i is the trajectory of (12) with initial condition $\xi(0) = \xi_0^i$, *i.e.* $\xi^i(t) = e^{Wt}\xi^i$. Finally, let $\mathscr{Y} = \{y_{\mathrm{ss}}^i(t)\}_{i=1}^{N_t} \subset \mathbb{R}$ denote the set of steady-state outputs of the ISWEC system (9), driven by each generated input u in terms of the set $\mathscr{I}$, *i.e.* $u^i(t) = [1\,1]\xi^i(t)$.

Remark 5. In practice, the steady-state output response $y_{\mathrm{ss}}(t)$ (which is always well-defined under the adopted assumptions) can be obtained as the output of (9) after a sufficiently large time $T_{\mathrm{ss}} \in \mathbb{R}^+$, *i.e.* after the transient response extinguishes.

Remark 6. By Lemma 2 (*i.e.* existence of the associated moment for the ISWEC device), given a (sufficiently small) initial condition ξ_0^i, producing an associated trajectory $\xi^i(t)$, the evaluation of the moment at $\xi^i(t)$ coincides with the well-defined steady-state output response of the ISWEC system (9).

By exploiting the connection highlighted in Remark 6, we propose the following data-driven strategy to compute Π in (15). Let $\mathcal{T} = \{t_q\}_{q=1}^{N_c} \subset [T_{\mathrm{ss}}, T_{\mathrm{ss}} + T_0]$, where each t_q represents a *time-instant*, with $N_c > N_t$. Let the set of constant matrices $\{\mathscr{M}_i\}_{i=1}^{N_t} \subset \mathbb{R}^{N \times N_c}$ and $\{\mathscr{O}_i\}_{i=1}^{N_t} \subset \mathbb{R}^{1 \times N_c}$ be defined such that

$$
\begin{aligned}
\mathscr{M}_i &= \begin{bmatrix} Z(\xi^i(t_1)) & Z(\xi^i(t_2)) & \dots & Z(\xi^i(t_{N_c})) \end{bmatrix}, \\
\mathscr{O}_i &= \begin{bmatrix} y_{\mathrm{ss}}^i(t_1) & y_{\mathrm{ss}}^i(t_2) & \dots & y_{\mathrm{ss}}^i(t_{N_c}) \end{bmatrix}.
\end{aligned}
\tag{16}
$$

With the definition of the matrices in (16), the approximated moment can be computed as $\tilde{\mathcal{M}}(\xi) = \Pi_{\mathrm{LS}} Z(\xi)$, where Π_{LS}

is the *unique* solution of the linear least-squares procedure:

$$
\Pi_{\mathrm{LS}} = \arg \max_{\Pi^\mathsf{T} \in \mathbb{R}^N} \left\| \Pi \begin{bmatrix} \mathscr{M}_1^\mathsf{T} \\ \mathscr{M}_2^\mathsf{T} \\ \vdots \\ \mathscr{M}_{N_t}^\mathsf{T} \end{bmatrix}^\mathsf{T} - \begin{bmatrix} \mathscr{O}_1^\mathsf{T} \\ \mathscr{O}_2^\mathsf{T} \\ \vdots \\ \mathscr{O}_{N_t}^\mathsf{T} \end{bmatrix}^\mathsf{T} \right\|_2^2,
\tag{17}
$$

subject to: $\Pi Z(0) = 0$.

Remark 7. The least-squares optimization method in (17) fully exploits the result of Lemma 3: Since $\mathcal{M}(\xi(t))$ is T_0-periodic, it is sufficient to use the information of the steady-state output response of (9) over a single single period, *i.e.* $[T_{\mathrm{ss}}, T_{\mathrm{ss}} + T_0]$, to fully characterise $\mathcal{M}(\xi(t))$. This, naturally, guarantees the well-posedness of the approximation proposed in (17).

Remark 8. The equality constraint in (17) is used to guarantee that the approximated moment effectively complies with the property in Remark 2.

VI. Case study

We now consider the ISWEC system described by the set of equations (9), with parameters as detailed in [5]. The approximation of the radiation system, *i.e.* the set of matrices (F, G, H) in (8), is computed using the moment-matching-based technique presented in [13], rendering an approximated system of dimension (order) $n_r = 6$. The total order of the state-space (9) is hence $n = 4 + n_r = 10$.

As anticipated in Section IV, we consider regular (monochromatic) input waves, with a fundamental period $T_0 = 2\pi/\omega_0$ [s], with ω_0 the associated fundamental frequency. In these conditions, the excitation input τ_{e} can be written as,

$$
\tau_{\mathrm{e}}(t) = \frac{|K_{\mathrm{e}}(\omega_0)|}{2} H_w \cos(\omega_0 t) = A_{\mathrm{e}} H_w \cos(\omega_0 t),
\tag{18}
$$

where H_w is the wave height, and $K_{\mathrm{e}} : \mathbb{R} \to \mathbb{C}$ defines the frequency-domain equivalent of the wave excitation impulse response mapping (see [12]).

Remark 9. The input in (18) can always be generated in terms of the signal generator (12), with a suitable selection for the output vector Q and initial condition $\xi(0)$. In this study, we set the former as $Q = A_{\mathrm{e}}[1\,1]$, while the latter is defined in terms of the wave height, *i.e.* $\xi(0) = H_w[0.5\ 0.5]^\mathsf{T}$.

From now on, we assume that the ISWEC is subject to waves such that $\omega_0 = 0.8$ [rad/s] (*i.e.* waves with a fundamental period of $T_0 \approx 8$ [s]), and $H_w \in \mathscr{H}$, with $\mathscr{H} = [0.3\,3]$ [m], so that a large variability with respect to the input amplitude is expected. Having knowledge of the operating conditions of the device, we now define the set of training initial conditions $\mathcal{I}_0$ as follows: Let $\{H_w^i\}_{i=1}^{N_t} \subset \mathscr{H}$ denote a finite set of N_t values for the wave height with a given spacing (*e.g.* uniform), and let each initial condition in the set $\mathscr{I}_0$ be hence defined as $\xi_0^i = H_w^i[0.5\ 0.5]^\mathsf{T}$. Note that, with such a definition, the computation of the sets $\mathscr{I}$ and $\mathscr{Y}$, *i.e.* signal generator trajectories and generator outputs, and corresponding steady-state outputs for system (9), can be performed directly.
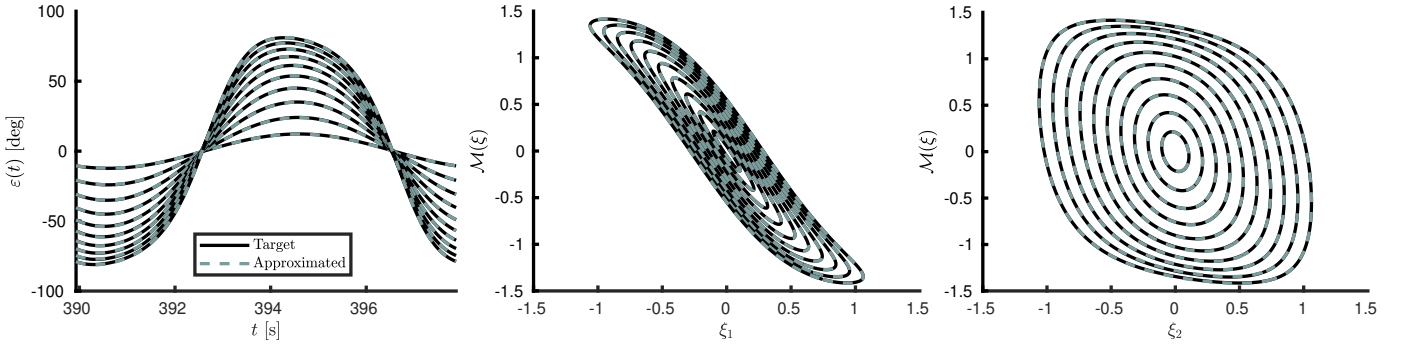
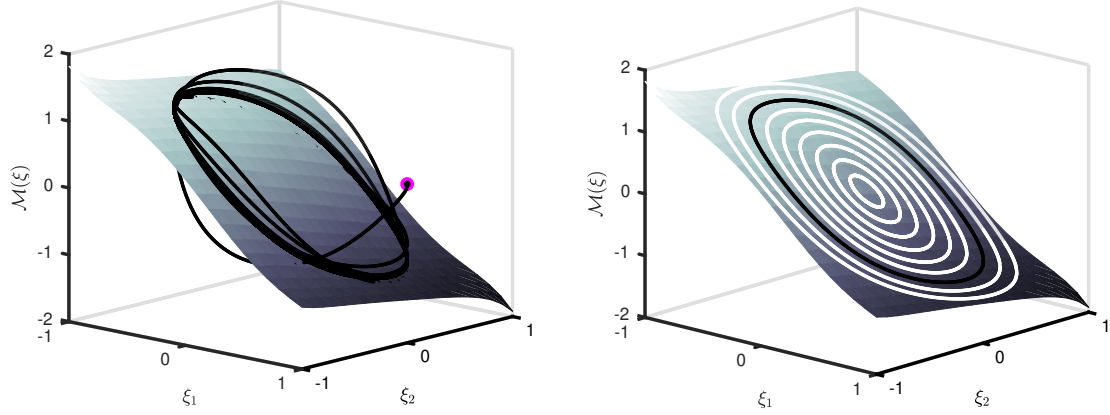Fig. 2. Approximation results for the set of training trajectories.

Fig. 3. Moment of the ISWEC system evaluated at a particular trajectory of the signal generator (including transient behaviour) with $H_w = 2.5$ [m], together with the approximated manifold (left); Target moment evaluated at the set of training trajectories, together with the approximated manifold (right).

With respect to the specification of Z in (15), and motivated by the degree of smoothness of π (see Remark 1), the definition of the approximation function space for the associated moment is done herein in terms of a polynomial surface in (ξ_1, ξ_2). In particular, we propose the following specification for Z:

$$Z(\xi) = \begin{bmatrix} \xi_2 & \xi_2^3 & \xi_2^5 & \xi_1 & \xi_1\xi_2^2 & \xi_1\xi_2^4 & \xi_1^2\xi_2 & \cdots \\ \xi_1^2\xi_2^3 & \xi_1^2\xi_2^5 & \xi_1^3 & \xi_1^3\xi_2^2 & \xi_1^3\xi_2^4 \end{bmatrix}^{\mathsf{T}} \quad (19)$$

where $Z(\xi) \in \mathbb{R}^{12}$. With the function space spanned by the terms in (19), and having computed the set of training initial conditions, training trajectories, and steady-state outputs from the response of (9), we proceed to implement the algorithm described in equation (17), resulting in an optimal expansion with

$$\Pi_{\mathrm{LS}} = \begin{bmatrix} -0.50 & -0.18 & 0.15 & -1.87 & 0.06 & -0.01 & \cdots \\ 0.24 & 0.25 & 0.01 & 0.57 & 0.09 & 0.06 \end{bmatrix}. \quad (20)$$

As can be appreciated in Figure 2 (left), the approximation (dashed) is well-behaved for all of the considered steady-state output responses (solid). Furthermore, as can be appreciated in Figure 2 (center and right), the approximated moment, computed along each specific training trajectory, is graphically indistinguishible from the target moment (computed in terms of each corresponding steady-state output), hence fully

demonstrating the performance of the data-driven approach for the training set.

The results presented in Figure 2 (particularly those in the center and right-hand-side plots), are extended in Figure 3. In particular, Figure 3 (left) shows the evolution of the moment of the ISWEC system, evaluated at a particular trajectory of the associated signal generator (including transient behaviour) with $H_w = 2.5$ [m], together with the manifold generated by the approximated moment (19). It can be readily appreciated how, after the transient period extinguishes, the target moment converges towards the approximated manifold, highlighting the performance of the approach for this case study. This is further extended in Figure 3 (right), where the target moment evaluated at the set of training trajectories, *i.e.* the results presented in 2 (center and right), are illustrated together with the approximated manifold for the complete operational space.

Finally, having demonstrated the accuracy of the approximated moment (19), we construct a reduced model for the ISWEC device based on (13), *i.e.*

$$\tilde{\Sigma} : \begin{cases} \dot{\Gamma} = \left(\begin{bmatrix} 0 & -0.8 \\ 0.8 & 0 \end{bmatrix} - \Delta \begin{bmatrix} A_{\mathrm{e}} & A_{\mathrm{e}} \end{bmatrix} \right) \Gamma + \Delta\tau_{\mathrm{e}}, \\ \tilde{y} = C\Pi_{\mathrm{LS}}Z(\Gamma), \end{cases} \quad (21)$$

with Z as in (19), Π_{LS} as in (20), and where the matrix Δ is such that we preserve the two dominant eigenvalues of the
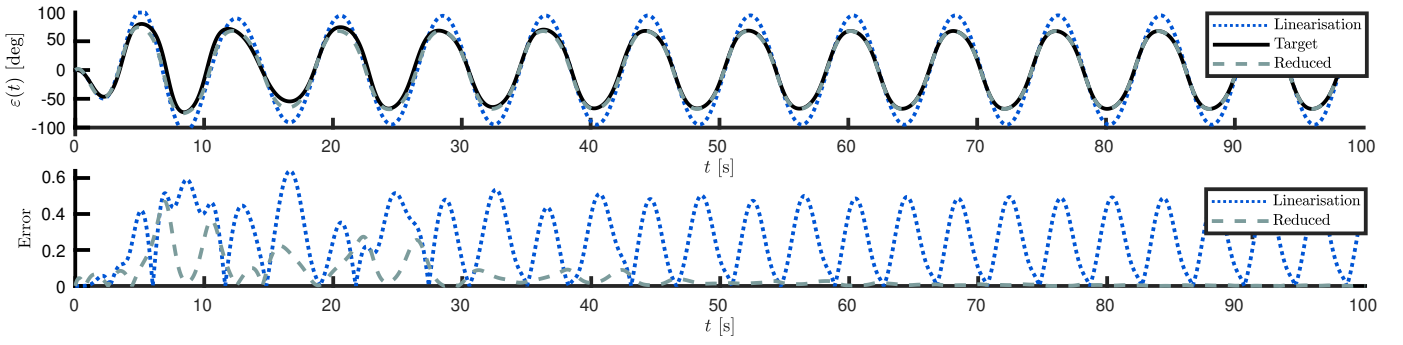
Fig. 4. Output traces for target ISWEC system, approximating model by moment-matching, and Jacobian linearisation (top); Absolute value of the difference between target system and reduced model by moment-matching, and target system and Jacobian linearisation (bottom).

associated Jacobian linearisation of the device, *i.e.* we choose Δ such that the eigenvalues of (21) are $\{-0.18 \pm j1.18\}$.

To illustrate the performance of the reduced model (21), Figure 4 (top) presents output traces for both the target (solid) ISWEC system (9), and the approximating (dashed) model (21), for a wave excitation torque corresponding with $H_w = 2.5$ [m]. In addition, the output corresponding with the Jacobian linearisation of (9) about the zero equilibrium is also presented (dotted), for the benefit of the reader. It can be apprecitaed that, after the transient period, both target and approximated responses are virtually identical. This is clearly not the case for the output arising from Jacobian linearisation, which presents a large error in both transient, and steady-state periods. This is further illustrated in Figure 4 (bottom), where time-traces of the absolute value of the difference between the output response of the target ISWEC system and each corresponding approximated output, are presented.

VII. CONCLUSIONS

Driven by the underlying necessity of control-oriented models for the optimization of the wave energy absorption process, we present, in this paper, a data-driven approach to model reduction by moment-matching for the ISWEC case. Such a methodology computes *linear* input-to-state models, with a nonlinear output map, by merely using data from system outputs for a defined class of inputs. The performance of the proposed technique is illustrated with detail, showing that the approach is capable of providing parsimonious models for control design, while successfully retaining steady-state response characteristics of the target ISWEC system, which are fundamental for energy-maximising control purposes.

ACKNOWLEDGMENT

REFERENCES

[1] J. V. Ringwood, G. Bacelli, and F. Fusco, "Energy-maximizing control of wave-energy converters: The development of control system technology to optimize their operation," *IEEE Control Systems*, vol. 34, no. 5, pp. 30–55, 2014.

[2] K. Ruehl and D. Bull, "Wave Energy Development Roadmap: Design to commercialization," *OCEANS 2012 MTS/IEEE: Harnessing the Power of the Ocean*, 2012.

[3] N. Faedo, G. Scarciotti, A. Astolfi, and J. V. Ringwood, "Nonlinear energy-maximizing optimal control of wave energy systems: A moment-based approach," *IEEE Transactions on Control Systems Technology (early access available)*, 2020.

[4] A. Battezzato, G. Bracco, E. Giorcelli, and G. Mattiazzo, "Performance assessment of a 2 dof gyroscopic wave energy converter," *Journal of Theoretical and Applied Mechanics*, vol. 53, no. 1, pp. 195–207, 2015.

[5] G. Bracco, M. Canale, and V. Cerone, "Optimizing energy production of an inertial sea wave energy converter via model predictive control," *Control Engineering Practice*, vol. 96, p. 104299, 2020.

[6] G. Scarciotti and A. Astolfi, "Nonlinear model reduction by moment matching," *Foundations and Trends in Systems and Control*, vol. 4, no. 3-4, pp. 224–409, 2017.

[7] A. Astolfi, G. Scarciotti, J. Simard, N. Faedo, and J. V. Ringwood, "Model reduction by moment matching: Beyond linearity a review of the last 10 years," in *2020 59th IEEE Conference on Decision and Control (CDC)*. IEEE, 2020, pp. 1–16.

[8] N. Faedo, F. J. D. Piuma, G. Giorgi, and J. V. Ringwood, "Nonlinear model reduction for wave energy systems: a moment-matching-based approach," *Nonlinear Dynamics*, vol. 102, no. 3, pp. 1215–1237, 2020.

[9] G. Scarciotti and A. Astolfi, "Data-driven model reduction by moment matching for linear and nonlinear systems," *Automatica*, vol. 79, pp. 340–351, 2017.

[10] A. Isidori, *Nonlinear control systems*. Springer Science & Business Media, 2013.

[11] M. Raffero, M. Martini, B. Passione, G. Mattiazzo, E. Giorcelli, and G. Bracco, "Stochastic control of inertial sea wave energy converter," *The Scientific World Journal*, vol. 2015, 2015.

[12] J. Falnes, *Ocean waves and oscillating systems: linear interactions including wave-energy extraction*. Cambridge university press, 2002.

[13] N. Faedo, Y. Peña-Sanchez, and J. V. Ringwood, "Finite-order hydrodynamic model determination for wave energy applications using moment-matching," *Ocean Engineering*, vol. 163, pp. 251 – 263, 2018.